Microfluidic tuning of distributed feedback quantum cascade lasers

L. Diehl, B.G. Lee, P. Behroozi, M. Lončar, M.A. Belkin, Federico Capasso

Division of Engineering and Applied Science
Harvard University
310 Cruft Laboratory
Cambridge, MA 02138, USA
ldiehl@deas.harvard.edu
capasso@deas.harvard.edu

T. Aellen, D. Hofstetter, M. Beck, J. Faist

Physics department
University of Neuchâtel
Rue A.-L. Breguet
2000 Neuchâtel, Switzerland

Abstract: In this Letter, we report the tuning of the emission wavelength of a single mode distributed feedback quantum cascade laser by modifying the mode effective refractive index using fluids. A fabrication procedure to encapsulate the devices in polymers for microfluidic delivery is also presented. The integration of microfluidics with semiconductor laser (optofluidics) is promising for new compact and portable lab-on-a-chip applications.

OCIS codes: (140.3070) Infrared and far-infrared lasers; (140.3600) Lasers, tunable.

References and links

1. F. Capasso, C. Gmachl, D.L. Sivco, and A.Y. Cho, "Quantum Cascade Lasers," Physics Today **55**, 34 (2002)
2. M. Beck, D. Hofstetter, T. Aellen, J. Faist, U. Oesterle, M. Ilegems, E. Gini and H. Melchior, "Continuous-wave operation of a mid-infrared semiconductor laser at room-temperature," Science **295** 301 (2002)
3. A. Evans, J. Nguyen, S. Slivken, J. S. Yu, S. R. Darvish, and M. Razeghi, "Quantum-cascade lasers operating in continuous-wave mode above 90ºC at λ~5.25 μm," Appl. Phys. Lett. **88**, 51105 (2006)
4. L. Diehl, D. Bour, S. Corzine, J. Zhu, G. Hofler, M. Lončar, M. Troccoli and F. Capasso, "High-power quantum cascade lasers grown by low-pressure metalorganic vapor-phase epitaxy operating in continuous wave above 400 K," Appl. Phys. Lett. **88**, 201115 (2006)
5. R. Maulini, A. Mohan, M. Giovannini, J. Faist, and E. Gini, "External cavity quantum-cascade lasers tunable from 8.2 to 10.4 um using a gain element with a heterogeneous cascade," Appl. Phys. Lett. **88**, 201113 (2006)
6. C. Gmachl, A. Straub, R. Colombelli, F. Capasso, D.L. Sivco A.M. Sergent and A.Y. Cho, "Single-mode, tunable distributed feedback and multiple wavelength quantum cascade lasers," IEEE J. Quantum Electron. **38**, 569 (2002).
7. A. Wittmann, M. Giovannini, J. Faist, L. Hvozdara, S. Blaser, D. Hofstetter, and E. Gini, "Room temperature, continuous wave operation of distributed feedback quantum cascade lasers with widely spaced operation frequencies," Appl. Phys. Lett. **89**, 141116 (2006).
8. S. Song, S.S.Howard, Z. Liu, A.O. Dirisu, C.F. Gmachl and C.B. Craig, "Mode tuning of quantum cascade lasers through optical processing of chalcogenide glass cladding," Appl. Phys. Lett. **89**, 41115 (2006).
9. A. Kosterev and F. Tittel, "Chemical sensors based on quantum cascade lasers," IEEE J. Quantum Electron. **38**, 582 (2002).
10. C. Charlton, F. de Melas, A. Inberg, N. Croitoru, and B. Mizaikoff, "Hollow-waveguide gas sensing with room-temperature quantum cascade lasers," IEE Proc. Optoelectron. **150**, 306 (2003)
11. J.Z. Chen, Z. Liu, C.F. Gmachl and D.L. Sivco, "Silver halide fiber-based evanescent-wave liquid droplet sensing with room temperature mid-infrared quantum cascade lasers," Opt. Express **13**, 5953 (2005)
12. B. Lendl, J. Frank, R. Schindler, A. Müller, M. Beck, and J. Faist, "Mid-infrared quantum cascade lasers for flow injection analysis," Anal. Chem. **72**, 1645 (2000)
13. J.Z. Chen, Z. Liu, Y.S. Rumala, D.L. Sivco, and C. Gmachl, "Direct cooling of room-temperature operated quantum cascade lasers," Electron. Lett. **42**, 534 (2005)

#73491 - $15.00 USD Received 14 September 2006; revised 7 November 2006; accepted 9 November 2006

14. M. Lončar, A. Scherer and Y. Qiu, "Photonic crystal laser sources for chemical detection," Appl. Phys. Lett. **82**, 4648 (2003).
15. D. Hofstetter, T. Aellen , M. Beck, and J. Faist, "High average power first-order distributed feedback quantum cascade lasers," IEEE Photon. Technol. Lett. **12**, 1610 (2000)
16. G.M. Whistesides, E. Ostuni, S. Takayama, X. Jiang and D.E. Ingberg, "Soft Lithography in Biology and Biochemistry," Annu. Rev. Biomed. Eng. **73**, 335 (2001)
17. Note that refractive indexes mentioned throughout this Letter correspond to the values known typically in the near-infrared ($\lambda \cong 2$ μm). According to our calculations, the refractive index change due to absorption resonances is less than 0.2 for all the liquids used. This result was found by applying the Kramers-Kronig relations to transmission measurements obtained with the different fluids used.
18. C.-B Kim and C. B. Su, "Measurement of the refractive index of liquids at 1.3 and 1.5 micron using a fiber optic Fresnel ratio meter," Meas. Sci. Technol. **15**, 1683 (2004)
19. C. Sirtori, J. Faist, F. Capasso, D. Sivco, A. Hutchinson, and A. Cho, "Quantum cascade lasers with plasmon enhanced waveguide operating at 8.4 μm wavelength," Appl. Phys. Lett. **66**, 3242 (1995).
20. M. Lončar, B.G. Lee and F. Capasso, unpublished

1. Introduction

Quantum Cascade Lasers (QCLs) are semiconductor lasers based on resonant tunneling and optical transitions between electronic levels confined in the conduction band of multi-quantum well structures. The emission wavelength of these devices can be adjusted by changing the width of a few quantum wells and spans continuously from 3.4 μm to 24 μm [1]. This spectral range corresponds to the "fingerprint" region of many molecules of interest in gas- or liquid-phase, which makes QCLs particularly interesting for spectroscopic applications. Another advantage of this technology is the fact that output power as large as hundreds of milliwatts can be routinely obtained from devices operating in continuous mode at room temperature [2, 3, 4]. Single mode operation with a narrow linewidth as well as good wavelength tunability are critical for gas sensing applications. For this purpose, high-performance external cavity (EC-)QCLs have been developed. Recently the continuous tuning of EC-QCLs over more 200 cm^{-1} was demonstrated at room-temperature [5]. Distributed feedback (DFB-)QCLs provide a more compact solution [6,7]. The frequency of DFB-QCLs can be efficiently tuned by varying the heatsink temperature, but this approach is however limited by the operating temperature range of the device. Recently, a non-thermal method to tune the emission wavelength of $\lambda \sim 7.9$ μm QCLs was demonstrated [8]. A device with an incorporated distributed Bragg reflector (DBR) was coated with a chalcogenide (As_2S_3) cladding layer. The deposition of the latter lead to a redshift of the QCL wavelength by 3.8 cm^{-1}. Furthermore, the illumination of the device with $\lambda \sim 368$ nm light resulted in a modification of the effective refractive index of the DBR grating as the refractive index of As_2S_3 can be increased with UV-light. An additional permanent redshift (1.31 cm^{-1}) of the QCL wavelength was achieved.

So far, QCLs have been used essentially for trace gas sensing in combination with multi-pass or photo-acoustic cells [9], allowing the detection of numerous gases at parts per million to parts per billions by volume levels. Alternative detection techniques include for example sensors based on hollow fibers [10]. Although it is very promising, only little work has been done to develop QCL-based techniques enabling the quantification of specific compound levels in liquids. All experiments reported in the literature are so far direct absorption measurements, in which the high power of QCLs is used to increase the sensitivity of the detection method [11,12]. Note that liquids have recently been used to help dissipating the heat in QCLs, enhancing at room temperature the maximum operating duty cycle of the devices investigated [13]. In this initial work, we report a novel way to integrate electrically pumped QCLs with microfluidic channels and demonstrate non-thermal wavelength tuning by varying the refractive index of liquid in direct contact with the laser. Note that similar results were obtained with optically pumped photonic crystal lasers in the near-infrared [14].

#73491 - $15.00 USD Received 14 September 2006; revised 7 November 2006; accepted 9 November 2006

2. Device fabrication and encapsulation

The devices used in this work are 1.5 mm long distributed feedback DFB-QCLs first reported in Ref. 15. The core of the laser waveguide is composed of a 1.75 μm thick active region based on a so-called diagonal transition design. The top cladding layer consists of a low-doped $In_{0.52}Ga_{0.47}As$ layer (Si, $1 \cdot 10^{17} cm^3$, thickness 2.2 μm) followed by a highly doped $In_{0.52}Ga_{0.47}As$ cap layer (Si, $1 \cdot 10^{19} cm^3$, thickness 0.7 μm). The Bragg grating, covering the entire ridge, was first defined holographically (period 1.6378 μm, n_{eff}=3.163) and etched in the cap layer (grating depth ~ 0.3 μm) before 34 μm wide ridges were wet etched. A thin layer of insulating Si_3N_4 was deposited on the sidewalls of the ridges. Electrical contacts were provided by narrow Ti/Au stripes evaporated at the edges of the ridges (see Fig. 1(a)). The conductivity of the highly doped cap layer is high enough to ensure an effective and homogeneous current injection in the gain medium. A more detailed description of the device geometry and the fabrication procedure can be found in Ref. 15. As shown on the sketch presented in Fig. 1(a), the top of the ridge is exposed to air, which allows a fraction of the mode to leak out in the air. Although the mode overlaps mostly with the semiconductor, replacing air by a liquid with a high refractive index n results in a relatively large tuning of the emission wavelength as described later in the text.

In order to deliver liquids to the sensitive part of the QCLs in a convenient and controlled manner, we developed a reliable and robust encapsulation procedure for building microcavities around lasers or other photonic devices. Ordinarily, poly-dimethyl-siloxane (PDMS) is the standard material for use in microfluidic applications due to the comparative ease of its molding process [16]. However, using PDMS for the fluid channel led to serious problems: as the wire bonds delivering power to the laser were also embedded in the PDMS, they would detach from the laser immediately if any external stress were applied. Hence, we developed a new technique to build the fluid cavity almost entirely out of SU-8 negative photoresist, so as to encase the wire bonds in a tough protective layer while still providing a leak proof device. The main steps of the fabrication process are illustrated in Fig. 1. First the laser chip without encapsulation is mounted on a Cu-submount, wire-bonded and tested (Fig. 1(b)). A 50 μm thick layer of Microposit SU-8 2050 (labeled SU-8 Layer 1 in Fig. 1(c)) is then spun on (2500 rpm, 30s) and soft-baked (65°C, 5min, then 95°C, 20min). Pre-coating with Microchem Omnicoat is optional (3000 rpm, 30s, followed by baking at 200°C for 1min). The SU-8 is exposed using a mask that protects the desired cavity region (shown as a dashed region in Fig. 1(c)), a very short region approximately ~ 100 μm wide at the front of the laser (as SU-8 is absorbing at the wavelength output of our lasers), and finally the gold electrical contacts on either side of the laser. The fluid cavity is approximately 5 mm long and its width is at most 6 mm. The SU-8 is then cross-linked (65°C for 1min, 95°C for 5min) and developed with PGMEA to wash away the unexposed regions. Using a microsyringe, Shipley S1818 positive photoresist is deposited in the cavity region. Surface tension keeps the photoresist from spilling over beyond the cavity edges. In addition, the same procedure is used to protect the front of the laser device. The S1818 need not be fully baked: only a thin protective skin has to form at its surface, and therefore the standard procedure of baking may be followed (105°C, 5min). In the next step, another 50 μm thick layer of SU-8 2050 (labeled SU-8 Layer 2 in Fig. 1(c)) is deposited, exposed with the exception that the mask no longer protects the cavity region and developed.

#73491 - $15.00 USD Received 14 September 2006; revised 7 November 2006; accepted 9 November 2006

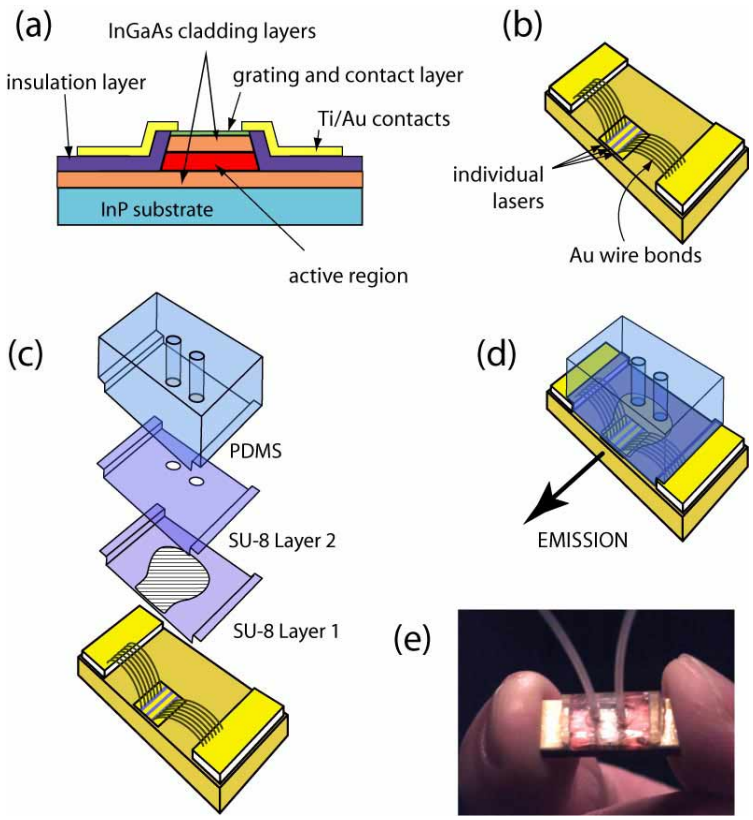

Fig. 1. (a) Schematic cross section of the processed DFB-laser. The current is injected laterally from two Ti/Au contacts. The Bragg grating is etched in the top layer composing the waveguide and is exposed to air/liquid. Diagrams showing (b) the laser as bonded and mounted on a Cu-heatsink, (c) different parts entering into the fabrication of the liquid chamber (note that the dashed area in the SU-8 layer1 is removed during the fabrication to form the fluid reservoir) (d) a device after encapsulation. Note that the tubing is not shown for clarity. (e) Picture of an encapsulated device.

This results in a hard covering forming over the photoresist-protected area. Degassed PDMS is then poured over the entire laser to form a layer several millimeters thick which is baked to a hard cure (65°C, 3 hours). PDMS sticks weakly to SU-8 and is therefore peeled off the device before being trimmed with a razor blade to reveal the electrodes and the front laser facet. The final shape of the PDMS block is shown in Fig. 1(c). Silicone potting cement (e.g., Loctite 5140) is then applied to the SU8. The trimmed PDMS layer is subsequently placed back on the laser and allowed to sit for 24 hours until the cement dries. 500 μm diameter holes are drilled in the PDMS over the fluid cavity all the way down to the copper substrate. PGMEA is subsequently used to entirely dissolve the photoresist used to fill the fluid cavity and to protect the front facet of the laser. After this step, both QCL facets are unobstructed or covered with material. Finally, tubing may be inserted into the drilled holes created, and fluid may be pumped into the fluid cavity for device testing. The final device (see Fig. 1(d) and (e)) is approximately 19 mm long, 7 mm wide and 8 mm tall after encapsulation.

#73491 - $15.00 USD Received 14 September 2006; revised 7 November 2006; accepted 9 November 2006

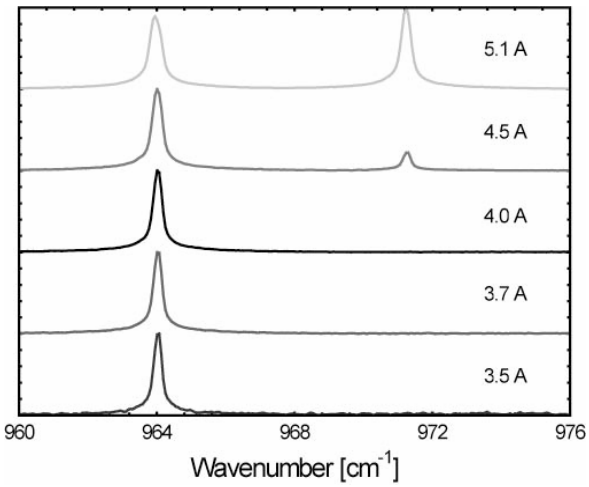

Fig. 2. Optical spectra obtained with an encapsulated device without liquid at room temperature and different current level.

3. Experimental results

After encapsulation, the lasers were tested in pulsed mode (5 kHz repetition rate, pulse length ~25 ns) at 300 K. The light output from the devices was sent either onto a calibrated thermopile detector for power measurements or into a Fourier-transform infrared spectrometer (Nicolet 860) equipped with a deuterated triglycine sulphate detector for spectral characterization. Figure 2 shows the optical spectra obtained with one of several encapsulated devices. The laser is clearly single mode close to threshold ($I_{threshold}$ = 3.1 A), and as the current increases, a second mode appears. The separation between the two modes is 7.1 cm^{-1} and corresponds to a higher order lateral mode. The current was kept at a constant value close to threshold (4.1 A) during the measurements with fluids, in order to ensure single mode operation of the laser. We note that the very short pulses and the very low duty cycle used during our experiment ensure that the electrical heating of the structure has only a very small effect on the optical spectrum. This can be seen from the data presented in Fig. 2.

Figure 3(a) shows the optical spectra obtained with fluids with different refractive index (immersion oils made by the company Cargilles) in the SU-8 chamber [17]. The measurements were performed in pulsed mode (repetition rate 5 kHz, pulse length ~25 ns) at 300 K at a constant current of 4.1 A. For simplicity, the liquids were delivered to the device using microsyringes attached to the tubing inserted in the PDMS. Before replacing a fluid with another one, the SU-8 chamber was cleaned thoroughly by flushing methanol and then dry air through it several times. A continuous and reproducible red shift of the wavelength was observed as the refractive index of the fluids was increased. Note that the spectral linewidth is of the order of 0.28 cm^{-1}, which corresponds to the resolution limit of our experimental set-up. Even in the presence of liquid, the optical spectrum remained clearly single mode, with a side-mode suppression ratio close to or better than 20 dB as shown in Fig. 3(b).

#73491 - $15.00 USD Received 14 September 2006; revised 7 November 2006; accepted 9 November 2006

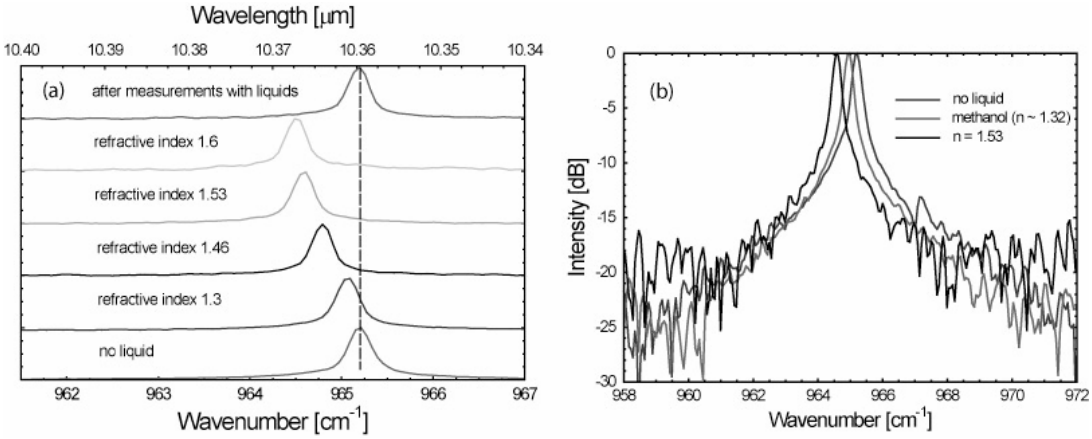

Fig. 3. (a) Optical spectra obtained at a fixed current (4.1 A) at room temperature with different liquids in the fluid chamber. The refractive index of the fluids varied from 1.3 to 1.735. (b) Optical spectra shown on a log scale measured without fluid, with the liquid with n = 1.53 and methanol.

The maximum wavelength tuning was obtained with the fluid having the largest refractive index and corresponds to 1.15 cm^{-1}. It is different from the value found before encapsulation of the device (0.8 cm^{-1}), i.e. when a drop of the same liquid was directly deposited onto the top of the laser with a micro-pipette. We do not have a clear explanation for the different tuning range observed before and after encapsulation. A layer of material with high refractive index might get deposited onto the DFB grating during the encapsulation procedure, pushing the optical mode towards the surface. This would result in an increase of the mode overlap with the fluids and as a consequence of the tuning range due to the presence of liquid. The magnitude of the discrepancy shows however that the encapsulation procedure does not affect dramatically the tuning range of the laser. The graph in Fig. 4 displays the experimentally observed wavelength shift as function of the refractive index and the results of calculations obtained using a two-dimensional finite difference time domain (FDTD) program. In our simple model, we assumed that the DFB grating has a 50% duty cycle and that the effective refractive index entering in the Bragg condition is given by the average of the effective refractive indexes calculated for the etched and non-etched structure. Fig. 4 shows that our data and the simulations follow the same trend. A red shift of the emission wavelength is clearly observed in both cases as function of refractive index. However, the magnitude of the shift is only in fair agreement. This difference can easily be explained by the simplicity of our model and the relatively large uncertainties in the various parameters (refractive index of the liquids [17], etch depth of the DFB grating, doping level (and as a consequence exact refractive index) of the different QCL layers) entering in the calculations. For example, the comparison between the experimental data and the calculations are better for deeper DFB grating (0.5 μm instead of 0.3 μm) as shown in Fig. 4. The agreement between the experiment and theory is sufficient to attribute the wavelength shift observed to an increase of the effective refractive index of the laser mode due to the presence of the liquid on the DFB grating.

A red shift was also observed when methanol was introduced in the fluid cavity. The emission wavelength measured was 964.94 cm^{-1}, which falls between the values found for the liquids with n=1.3 and n=1.46. This observation indicates that the refractive index of methanol can be assumed to be within this range of refractive index, in fair agreement with the value found in Ref. [18] (n=1.32).

#73491 - $15.00 USD Received 14 September 2006; revised 7 November 2006; accepted 9 November 2006

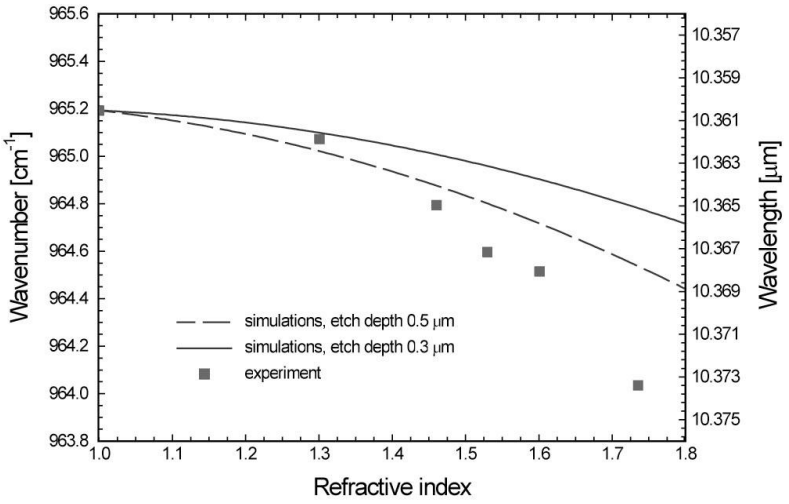

Fig. 4. Comparison between the peak position obtained experimentally from the data shown in Fig. 3(a) and the results of FDTD simulations.

Figure 5(a) shows the voltage and light intensity vs. current curves (V-I and L-I) obtained with a second encapsulated laser. Its spectral properties are quantitavely and qualitatively similar to those described in Fig. 2, 3 and 4. These V-I and L-I curves were taken with and without liquid in the SU-8 chamber and under the same conditions as used for the spectral characterization, i.e. in pulsed mode at 300 K. The optical power was measured with a calibrated thermopile detector. The V-I curves are not affected by the liquids since the latter are not conductive. The same conclusions were reached when the devices were tested electrically with deionized water and methanol. On the contrary, the L-I curves are clearly modified as seen on Fig. 5(a). The threshold current density increases consistently when liquids with increasing refractive index were pumped into the SU-8 chamber. This change cannot be explained by an absorption in the liquid as the most transparent fluid used actually had the highest refractive index. The increase in threshold current density can be explained by the fact that the laser backfacet is immersed in the liquid, resulting in the lowering of the reflectivity of the mirror facet and thus an increase of the mirror losses. A change of threshold current density obtained by varying the mirror losses can be used to determine the waveguide losses of the laser [19]. The waveguide losses deduced from the data presented in Fig. 5(a) are equal to 18.3 cm^{-1}, which is comparable to the calculated value (24.6 cm^{-1}).

The temperature tuning coefficient for the DFB QCL used is equal to $\Delta\nu/\Delta T$=-0.063 cm^{-1}/K [15]. The amount of tuning that we report in the present letter can be obtained simply by varying the heatsink temperature by less than 15 K. However, the tuning caused by the fluids is essentially limited by the very small (approximately 0.01 %) fraction of the optical mode propagating in the liquid. The overlap can be improved greatly by changing the geometry of the laser, e.g. by reducing the width of a ridge waveguide QC laser and leaving the sidewalls uncovered with metal. A QCL structure with a special cavity based on a photonic crystal has been proposed recently. The novelty of this design is the fact that the holes are placed in the plane perpendicular to the growth axis. The tuning range of this device is expected to be close to $\Delta\nu/\Delta n$=100 cm^{-1} [20].

#73491 - $15.00 USD Received 14 September 2006; revised 7 November 2006; accepted 9 November 2006

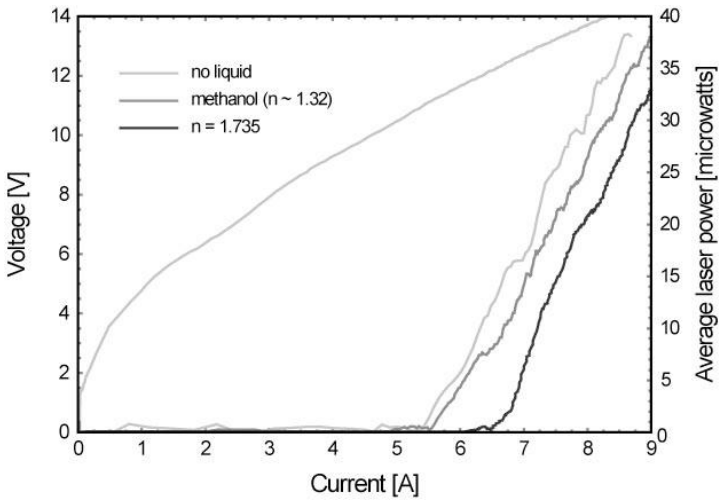

Fig. 5. (a) Voltage and output power vs. current curves obtained at room temperature with different liquids in the fluid chamber. Note that these data were obtained with an encapsulated DFB QCL different from the one used to produce the data shown in Fig. 2, 3 and 4.

In this initial work we have concentrated on demonstrating the on-chip integration of microfluidics with quantum cascade lasers by tuning single mode devices via changes of the effective refractive index of the mode induced by fluids. The accuracy and the reliability of this approach need to be further investigated and improved before the device can be implemented for any practical chemical sensing applications.

In the future, we also plan to explore QC lasers with integrated microfluidic delivery of analytes *in-situ* (either in intimate contact with the laser ridge, as in the present study, or into the laser cavity itself through via-*holes)* based on mid-ir *absorption* changes (rather than refractive index variations) induced by the analytes. This type of chemical detection should be particularly sensitive and could lead to the *detectorless ir* spectroscopy by monitoring the current-voltage characteristic changes of the laser.

Acknowledgments

The Harvard group acknowledges financial support from DARPA (optofluidic center) under grant number HR0011-04-1-0032. The center for Nanoscale systems (CNS) at Harvard University is also gratefully acknowledged. Harvard-CNS is a member of the National Nanotechnology Infrastructure Network (NNIN). Fruitful discussions with Prof. O. Painter and his group (Caltech) are also acknowledged.

#73491 - $15.00 USD Received 14 September 2006; revised 7 November 2006; accepted 9 November 2006